

SIZE EFFECT AND STABILITY OF FRACTURE

B. Trunk, H. Sadouki, and F.H. Wittmann,
Laboratory for Building Materials,
Swiss Federal Institute of Technology Zurich, Switzerland

Abstract

The effect of the specimen length on the tensile strength and on the stability of the fracture process in direct tension is investigated. Tests have been carried out on cylindrical specimens with a constant cross section but with different length. It was found that the tensile strength decreases with increasing specimen length. The influence of the strain softening behaviour on the stability of fracture is discussed.

1 Introduction

Tensile strength, specific fracture energy, and strain softening have proved to be material parameters which allow us to describe crack formation and propagation in concrete in a realistic way. Soon it was found, however, that these parameters depend on both specimen size and geometry. Weibull (1939) proposed a statistical theory that applies the weakest link concept to the strength of solids. Freudenthal (1968) linked this theory

with the Griffith crack instability criterion (Griffith (1921)). A stochastic theory for concrete fracture under different types of loading, in which, not only the stochastic characteristics of the process, but also the statistical stress distribution due to the material defects are taken into consideration was proposed by Mihashi and Masanori (1977) and Mihashi and Wittmann (1980). Another concept is the size-effect law proposed by Bazant (1983) that is applicable for geometrically similar structures of different size. It describes the transition from the strength theory, according to which failure occurs at a constant stress level, to the LFM. The failure criterion is expressed in terms of the energy consumed per unit crack length. The multifractal scaling law as proposed by Carpenteri et al. (1993) and Carpenteri and Ferro (1994) is based on the assumption of multifractality for the damaged microstructure of the material. However, all these models do not consider the limit of stability.

For practical applications a clear distinction must be made between stable and unstable failure. Direct tension tests with the same cross section but different specimen length were carried out to determine the limit of stable fracture.

2 Background

In order to characterize the ductility of a material Petersson (1981) introduced a characteristic length l_{ch} and a critical length l_{crit} as material parameters:

$$l_{ch} = \frac{E \cdot G_f}{f_t^2} \quad \text{and} \quad l_{crit} = 2 \cdot l_{ch} = \frac{2 \cdot E \cdot G_f}{f_t^2} \quad (1)$$

When the maximum load in direct tension is reached and the elastic strain energy stored in the specimen exceeds the capability of energy consumption of the fracture process zone, the material will fail in a brittle way. This means that in a specimen with a constant cross section and a length of $2 \cdot l_{ch}$ brittle failure will occur. The stability limit given by eq. 1 is based on the assumption that the loading system is infinite stiff.

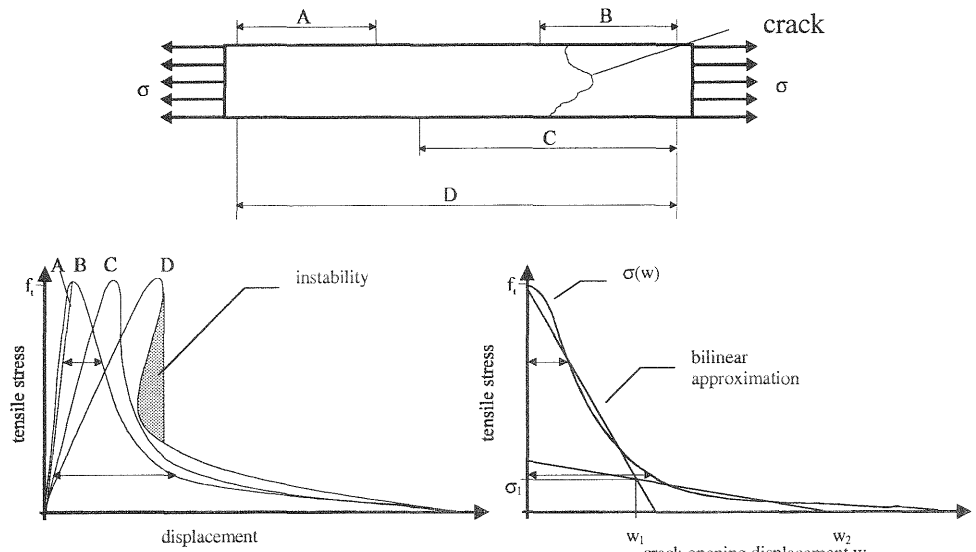


Fig. 1. Instability and snap back in direct tensile tests

We can assume that instability will occur when the slope of the softening diagram is equal or greater than the stiffness of the total loading system. Fig. 1 illustrates a direct tension test. The displacement is recorded by the four displacement transducers A, B, C and D. In the critical state when the slope of the decreasing part of the stress displacement diagram tends towards minus infinity the material will fail in a brittle way (displacement transducers C). The corresponding specimen length is called the critical length l_{crit}^* . For a known softening diagram $\sigma(w)$ (see Fig 1) as obtained from a stable test and an infinite stiff loading system the critical length l_{crit}^* can be calculated by eq. 2:

$$l_{crit}^* = \frac{E}{\left. \frac{\partial \sigma(w)}{\partial w} \right|_{\min}} \quad (2)$$

Where E is the modulus of elasticity of the specimen and w the crack opening displacement. If we assume a bilinear softening diagram (see Fig. 1) eq. 2 can be rewritten as:

$$l_{crit}^* = \frac{E \cdot w_1}{f_t - \sigma_1} \quad (3)$$

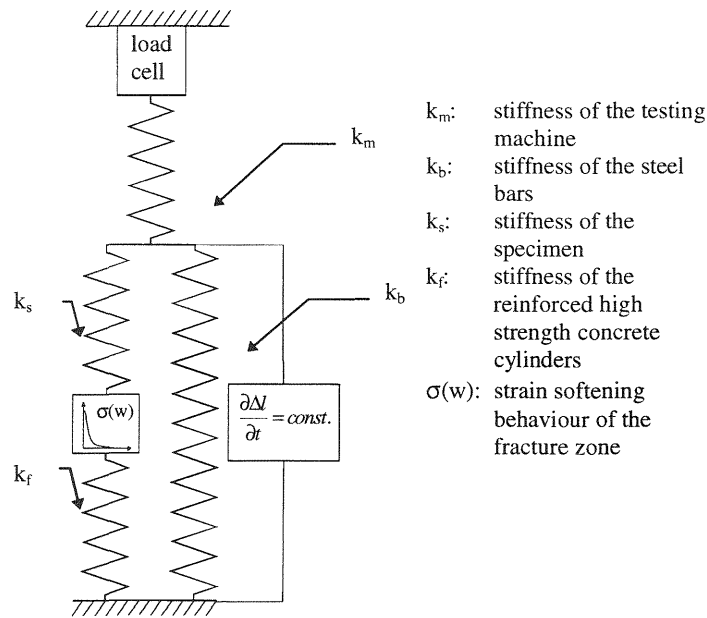


Fig. 2. Schematic illustration of the direct tension test with parallel stretched steel bars

For direct tension tests Petersson (1981) proposed among others not only the use of a stiff testing machine but also the use of steel bars attached parallel to the specimen to increase the stiffness of the total loading system. In Fig. 2 the schematic illustration of the direct tension test set-up used in this project is shown. The specimen load $F_s(\Delta l)$ can be determined from the measured load $F_m(\Delta l)$, the displacement Δl , and the stiffness of the steel bars k_b by the following equation:

$$F_s(\Delta l) = F_m(\Delta l) - k_b \cdot \Delta l \quad (4)$$

The crack opening w after peak load can be calculated by the following equation:

$$w = \Delta l - \frac{k_s + k_r}{k_s \cdot k_r} \cdot F_s(\Delta l) \quad (5)$$

Where $\frac{k_s + k_r}{k_s \cdot k_r} \cdot F_s(\Delta l)$ represents the displacement of the undamaged parts of the specimen and the reinforced high strength concrete cylinders.

To determine the critical length l_{crit}^m using the finite stiff loading system shown in Fig. 2 the critical length l_{crit}^* (see eq. 2) must be corrected by the following terms according to Petersson (1981):

$$l_{crit}^m = l_{crit}^* - \frac{E_s \cdot A}{k_b + k_m} - \frac{E_s}{E_f} \cdot l_f \quad (6)$$

Where E_s is the modulus of elasticity and A the cross section of the specimen, E_f the modulus of elasticity of the high strength concrete, and l_f the length of the reinforced high strength concrete cylinders. To determine the critical length l_{crit}^* from the test data eq. 6 leads to the following correction factor l_{corr} that represents an additional virtual specimen length:

$$l_{corr} = \frac{E_s \cdot A}{k_b + k_m} + \frac{E_s}{E_f} \cdot l_f \quad (7)$$

Fig. 3 shows the correction factor as a function of the stiffness of the total loading system for a specimen diameter of 100 mm and a Young's modulus of 40000 N/mm². The length of the reinforced high strength concrete cylinders is neglected.

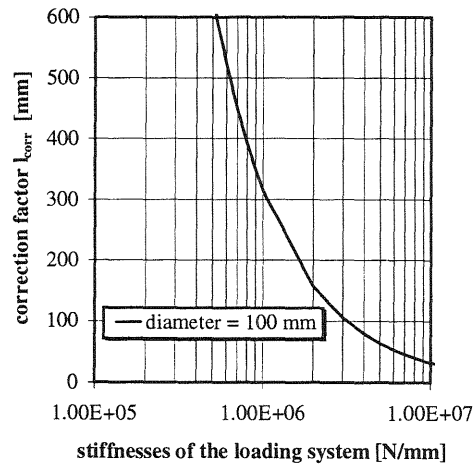


Fig. 3. Correction factor as a function of the stiffness of the loading system for a specimen diameter of 100 mm according to eq. 7

3 Experiments and results

3.1 Test set-up

The aim was to load cylindrical specimens with different length in a uniaxial direct tensile test. To achieve a homogeneous uniaxial stress distribution all over the specimen it was necessary to avoid stress concentrations at the loading interface. The attachments to the loading machine have to be restrained against rotation. Otherwise the post peak path of the load deflection curve bifurcates (Bazant et al. (1993)). However, due to the relative brittleness of concrete a very stiff testing machine has to be used for determining the strain softening behaviour (Petersson (1981)).

The test specimens were glued to reinforced high strength concrete supporting cylinders with approximately the same contraction of the endface to avoid shear stresses. Both, the specimen and the high strength concrete cylinders, have the same diameter. An epoxy resin based bicomponent adhesive was chosen. The reinforced high strength concrete cylinders were glued into flanged fittings as shown in Fig. 4. Here the same adhesive was chosen. The flanged fittings were screwed on steel supporting plates for rotational stiff attachment to the testing machine.

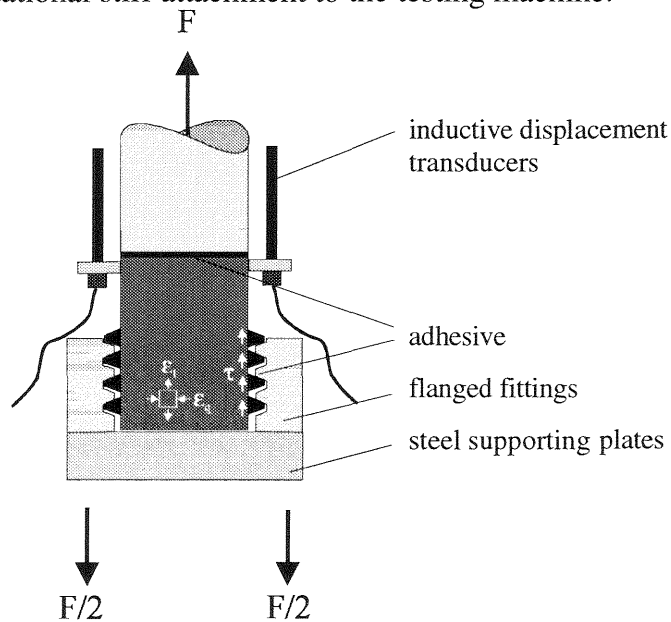


Fig. 4. Specimen bearing for direct tensile tests

Fig. 5 shows the set-up for the direct tensile tests. Steel bars were attached parallel to the specimen in order to increase the stiffness of the

machine. The tests were run under displacement controlled conditions $\partial\Delta / \partial t = const.$ using a servo-hydraulic testing machine.

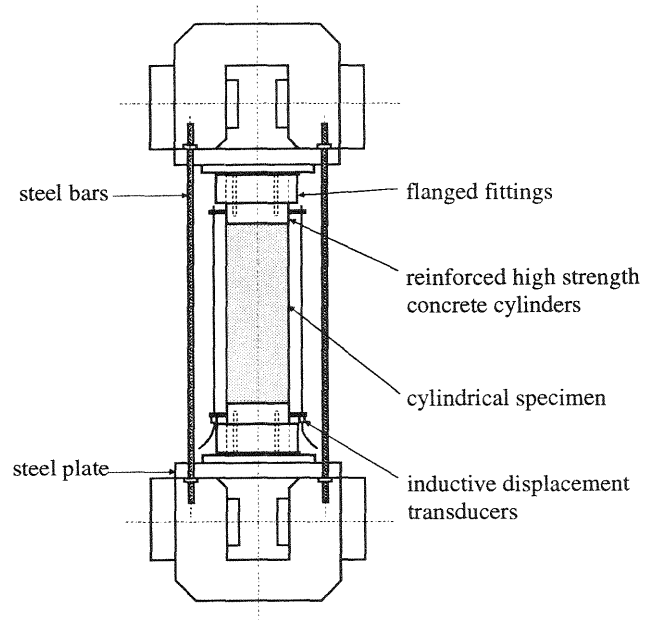


Fig. 5. Set-up for direct tension tests with a servo-hydraulic testing machine

3.2 Preparation of specimens

The concrete used for casting the specimens was made with a maximum grain size of 32 mm, a cement content of 300 kg/m^3 and a water/cement ratio of 0.5. The resulting compressive strength after 28 days was 49.7 N/mm^2 , the modulus of elasticity was 38800 N/mm^2 and the density 2430 kg/m^3 . The specimens were stored three and a half years at 70 % relative humidity and $20 \text{ }^\circ\text{C}$. The diameter of the specimens was kept constant at 100 mm and the length varied between 50 and 400 mm.

3.3 Results

Direct tension tests were carried out in order to determine the material fracture mechanics parameters and the critical length of stability of fracture. The mean stress-displacement curves for stable tests and all curves for the instable tests are shown in Fig. 6. The results of the tests are summarized in Table 1.

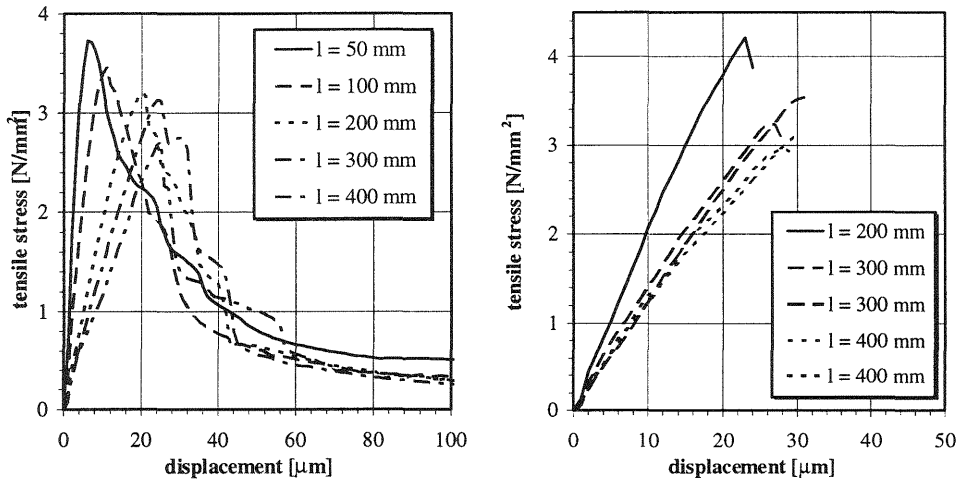


Fig. 6. Stable and unstable stress-displacement curves as observed in direct tension tests

Table 1. Test results

specimen length [mm]	50	100	200	300	400
tensile strength f_t [N/mm^2]	3.82	3.58	3.55	3.44	2.95
fracture energy [N/m]	220	170	160	140	170
number of stable tests	2	3	3	2	1
number of unstable tests	0	0	1	2	2

4 Evaluation of results and discussion

Fig. 7 shows the experimental softening curves and the bilinear approximation. In Table 2 the bilinear fracture mechanics parameters as determined from all stable tests are given. The parameters of the approximation were obtained by a non-linear least square fit. In Table 2 the characteristic and the critical length l_{ch} and l_{crit} calculated by eq. 1 and the critical length l_{crit}^* calculated by eq. 3 are given in addition.

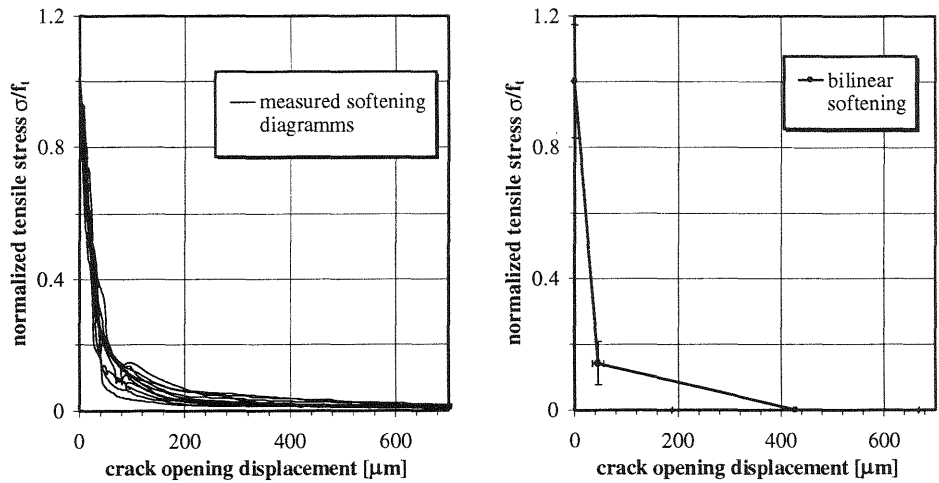


Fig. 7. Experimental softening curves and bilinear approximation

Table 2. Fracture mechanics parameters

Bilinear softening				characteristic and critical lengths		
f_t [N/mm ²]	σ_1 [N/mm ²]	w_1 [mm]	w_2 [mm]	l_{ch} [mm]	l_{crit} [mm]	l_{crit}^* [mm]
3.12	0.44	0.046	0.428	568	1136	597

The values of the measured tensile strength f_t are plotted in Fig. 8 against the specimen length. In accordance with the Weibull theory, tensile strength decreases with increasing specimen length. Under simplifying assumptions the following expression can be obtained from Weibull theory:

$$\left(\frac{f_t}{f_{t,0}} \right) = \left(\frac{l_0}{l} \right)^{\frac{1}{m}} \quad (8)$$

The parameters in eq. 8 have been determined by a least square fit to be:

$$m = 11.8$$

$$l_0 = 50 \text{ mm}$$

$$f_{t,0} = 3.82 \text{ N/mm}^2$$

The probability for brittle fracture as a function of the corrected specimen length calculated by eq. 7 is shown in Fig. 9.

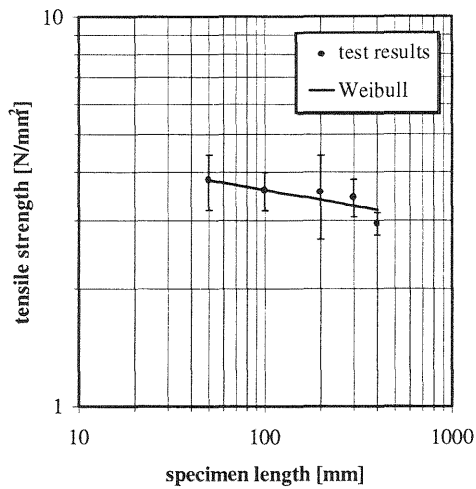


Fig. 8. Tensile strength as function of length

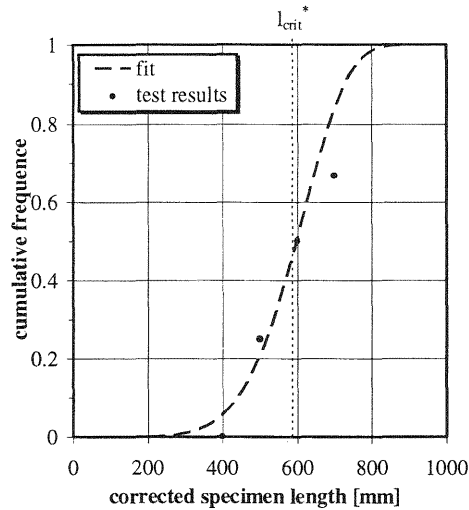


Fig. 9. Cumulative distribution function for instability

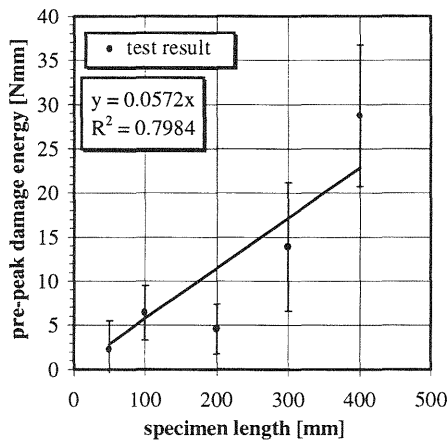


Fig. 10. Pre-peak damage energy as function of the specimen length

The pre-peak damage energy G_p introduced by Sadouki (1995) also increases with increasing specimen volume (i.e. length). To eliminate the influence of the differing tensile strength the pre-peak damage energy is calculated for each specimen length by using a stress corresponding to the lowest mean tensile strength ($l = 400$ mm). The results are shown in Fig. 10. The dependence on the specimen length can be described by the following linear function:

$$G_p = k \cdot l \quad (9)$$

with $k = 0.0572 \text{ N}$, G_p is the pre-peak damage energy, and l the specimen length. It can be assumed, that within the experimental scatter the pre-peak damage energy is homogeneously distributed all over the specimens volume.

5 Conclusions

It has been shown that the critical length l_{crit} not only depends on the fracture energy G_f the tensile strength f_t and the modulus of elasticity E , but also on the shape of the softening diagram. That means, that the slope at the inflection point of the strain softening diagram is responsible for the stability of crack propagation. The slope of the first branch of the bilinear diagram can be used as a first approximation. The specimen length not only influences the stability but also the tensile strength and the pre-peak damage energy.

References

- Bazant, Z.P. (1984) Size effect in blunt fracture: concrete, rock, metal. **Journal of Engineering Mechanics**, 110 (4), 518 - 535.
- Bazant, Z.P. and Cedolini, L. (1993) Why direct tension test specimens break flexing to the side. **Journal of Structural Engineering**, 119 (4), 1101 - 1113.
- Carpinteri, A., Chiaia, B., and Ferro, G. (1993) Multifractal scaling law for the nominal strength variation of concrete structures, in **Size effect in concrete structures**, Sendai, Japan, 173 - 186.
- Carpinteri, A. and Ferro, G. (1994) Size effect on tensile fracture properties: a unified explanation based on disordered fractality of concrete microstructures. **Materials and Structures**, 27, 563 - 571.
- Freudenthal, A.M. (1968) Statistical approach to brittle fracture, in **Fracture** (ed. H. Libowitz), 2, Academic Press, New York, 591 - 619.

- Griffith, A.A. (1921) The phenomena of rupture and flow in solids. **Phil. Trans. R. Soc.**, 221, London, 163 - 198.
- Mihashi, H. and Masanori, I. (1977) A stochastic theory for concrete fracture. **Cement and Concrete Research**, 7, 411 - 422.
- Mihashi, H. and Wittmann, F.H. (1980) Stochastic approach to study the influence of rate of loading on strength of concrete. **Heron**, 25 (3).
- Petersson, P.E. (1981) Crack growth and development of fracture zones in plain concrete and similar materials. Report TVBM-1006, Lund Institute of Technology, Lund, Sweden.
- Sadouki, H. and Wittmann, F.H. (1995) Numerical concrete applied to investigate size effect and stability of crack propagation, in this volume.
- Weibull, W. (1939) A statistical theory of strength of materials, Swedish Royal Institute for Engineering, 151, Stockholm, 591 - 619.